

# Is there an exoplanet in the Solar System?

Alexander J. Mustill<sup>1\*</sup>, Sean N. Raymond<sup>2,3</sup> and Melvyn B. Davies<sup>1</sup>

<sup>1</sup>*Lund Observatory, Department of Astronomy & Theoretical Physics, Lund University, Box 43, SE-221 00 Lund, Sweden*

<sup>2</sup>*CNRS, Laboratoire d’Astrophysique de Bordeaux, UMR 5804, F-33270, Floirac, France*

<sup>3</sup>*Univ. Bordeaux, Laboratoire d’Astrophysique de Bordeaux, UMR 5804, F-33270, Floirac, France*

Accepted XXX. Received YYY; in original form ZZZ

## ABSTRACT

We investigate the prospects for the capture of the proposed Planet 9 from other stars in the Sun’s birth cluster. Any capture scenario must satisfy three conditions: the encounter must be more distant than  $\sim 150$  au to avoid perturbing the Kuiper belt; the other star must have a wide-orbit planet ( $a \gtrsim 100$  au); the planet must be captured onto an appropriate orbit to sculpt the orbital distribution of wide-orbit Solar System bodies. Here we use N-body simulations to show that these criteria may be simultaneously satisfied. In a few percent of slow close encounters in a cluster, bodies are captured onto heliocentric, Planet 9-like orbits. During the  $\sim 100$  Myr cluster phase, many stars are likely to host planets on highly-eccentric orbits with apastron distances beyond 100 au if Neptune-sized planets are common and susceptible to planet–planet scattering. While the existence of Planet 9 remains unproven, we consider capture from one of the Sun’s young brethren a plausible route to explain such an object’s orbit. Capture appears to predict a large population of Trans-Neptunian Objects (TNOs) whose orbits are aligned with the captured planet, and we propose that different formation mechanisms will be distinguishable based on their imprint on the distribution of TNOs.

**Key words:** Kuiper Belt: general — planets and satellites: dynamical evolution and stability — planets and satellites: individual: Planet 9 — planetary systems — open clusters and associations: general

## 1 INTRODUCTION

Recent speculation suggests that the outer Solar System hosts a “Planet 9” of several Earth masses or greater. [Trujillo & Sheppard \(2014\)](#), in announcing the discovery of an unusual trans-Neptunian object (TNO) of high perihelion (2012 VP<sub>113</sub>), noticed a clustering of the argument of perihelion of bodies lying beyond  $\sim 150$  au, and attributed this to a hypothetical super-Earth body lying at several hundred au whose gravity dominates over the perihelion precession induced by the known planets that would cause an orbital de-phasing over 100s of Myr. This argument has been developed by [de la Fuente Marcos & de la Fuente Marcos \(2014\)](#), who proposed two distant planets to explain further patterns in the distributions of orbital elements. [Malhotra et al. \(2016\)](#) point out mean-motion commensurabilities between the distant TNOs, which they trace back to a hypothetical body at  $\sim 665$  au whose resonant perturbations on the TNOs would lead to their apsidal confinement. Earlier work was summarized and extensively developed by [Lykawka &](#)

[Mukai \(2008\)](#), who favoured a sub-Earth mass embryo at 100 – 200 au.

Current interest has been fomented by [Batygin & Brown \(2016\)](#), who show numerically and analytically how the apsidal and nodal clustering of the distant TNOs arises as a result of resonant and secular dynamical effects from a distant perturber. They identify a range of semi-major axes (400 – 1500 au) and eccentricities (0.5 – 0.8) for which a distant planet can explain the orbital elements of the distant TNOs<sup>1</sup>. This range of semi-major axes is more distant than proposed by [Trujillo & Sheppard \(2014\)](#) and [de la Fuente Marcos & de la Fuente Marcos \(2014\)](#), but brackets the resonant perturber of [Malhotra et al. \(2016\)](#). The latter authors favour a lower eccentricity for Planet 9, but as the range proposed by [Batygin & Brown \(2016\)](#) is backed up by multi-Gyr numerical simulations, we adopt their ranges of  $a$  and  $e$  as orbital elements of Planet 9 in this paper. Unfortunately, observations currently do not constrain the possible orbit very strongly. Sub-Neptune mass bodies can

\* E-mail: alex@astro.lu.se

<sup>1</sup> A follow-up study ([Brown & Batygin 2016](#)) slightly refines these parameters, disfavouring the wider orbits.

exist undetected in EM emission at several hundred au (Luhman 2014; Ginzburg et al. 2016; Linder & Mordasini 2016), while Fienga et al. (2016) show that a dynamical analysis of Cassini ranging data may rule out some ranges of orbital phase for a Planet 9, although they restricted their analysis to only a single choice of  $a$  and  $e$ . Henceforth, we consider the whole of the parameter space identified by Batygin & Brown (2016) to be viable.

In this paper we investigate how the Solar System might have come to host a wide-orbit eccentric body such as Planet 9, a class of object we refer to as “Novenitos”. A number of lines of evidence suggest that the Sun formed in a sizeable cluster of a few thousand stars (see Adams 2010; Pfalzner et al. 2015, for reviews), and previous dynamical studies have shown that orbiting bodies at large radii can be transferred between stars in the slow ( $\sim 1 \text{ km s}^{-1}$ ) close encounters typical in open clusters (Malmberg et al. 2011; Belbruno et al. 2012; Jílková et al. 2015); and we show that it is indeed possible for the Sun to have captured such a planet from another star in a close encounter in its birth cluster. Our study is complementary to the recent work of Li & Adams (2016), who also identify capture in a cluster as a possible source for Planet 9. Whereas these authors consider the capture of planets initially on circular or moderately-eccentric orbits, we focus on a scenario in which the Sun captures a highly-eccentric planet with a semi-major axis of several hundred au but a pericentre of  $\sim 10$  au. In Section 2 we present our simulations for the capture of eccentric planets by the Sun; we show how suitable source planets may exist on highly eccentric orbits around their parent star for many Myr during eras of planet–planet scattering in Section 3; and we discuss our results in Section 4.

## 2 CAPTURE OF NOVENITOS IN A FLYBY

We first consider the likelihood of the capture of a wide-orbit planet by the Sun in a close encounter with another star. Capture can occur when the initial orbital velocity of the planet around its original host, the final orbital velocity of the planet around the Sun, and the velocity of the encounter, are all comparable. For the postulated orbit of Planet 9 of  $\sim 1000$  au, this suggests a similarly wide orbit around the original host (unless the host is low mass, in which case smaller orbits become favoured) and an encounter velocity of  $\sim 1 \text{ km s}^{-1}$ . Given this velocity, we constrain the impact parameter by requiring that the cold classical Kuiper Belt not be disrupted during the flyby. This requires a perihelion separation greater than  $\sim 150$  au (Breslau et al. 2014), or an impact parameter greater than 500 au, depending on the mass of the original host. For transfer of material between stars, the minimum separation must also be at most the semi-major axis of the orbiting bodies, meaning a perihelion separation  $\lesssim 1000$  au for the close encounter. Fortunately for the capture hypothesis, these encounters occur remarkably frequently in clusters of a few hundred stars or more: Malmberg et al. (2007, 2011) found that only  $\sim 20\%$  of Solar-mass stars in a cluster of  $N = 700$  avoid a close encounter within 1000 au, and the mean minimum perihelion distance is  $\sim 250$  au; similarly, Adams et al. (2006) found an encounter rate of 0.01 encounters within  $\sim 300$  au per star per Myr in an  $N = 1000$  subvirial cluster.

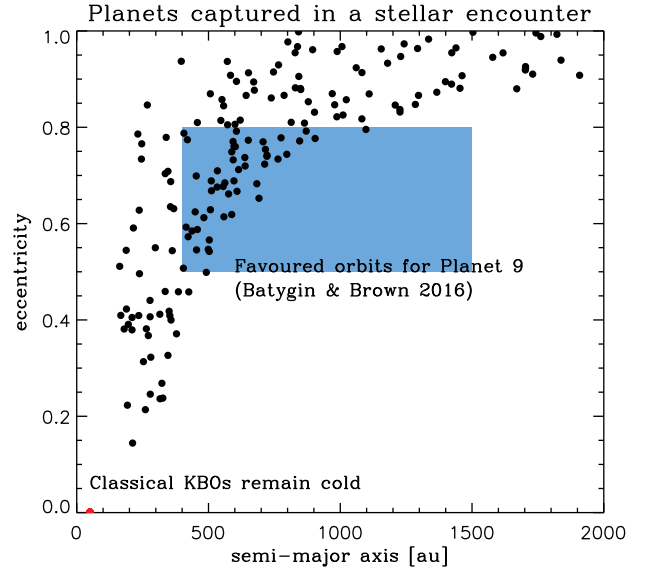


**Figure 1.** Semi-major axes and eccentricities of particles after a flyby with  $M_{\star} = 0.1M_{\odot}$ ,  $b = 1000$  au,  $v_{\text{inf}} = 5 \times 10^{-4} \text{ au d}^{-1}$ , and initial orbits of  $a = 100$  au,  $q = 10$  au around the star. The orbits of captured particles around the Sun are shown in black, while the blue box marks the range for Novenitos, following Batygin & Brown (2016). In red, at the lower left corner, are the post-flyby orbits of the barely-perturbed Kuiper Belt Objects, initially on circular orbits at 50 au from the Sun.

**Table 1.** Parameter choices for our flyby simulations.

Parameter	Values
Mass of intruder $M_{\star}$	{0.1, 0.2, 0.5, 1.0, 1.5} $M_{\odot}$
Impact parameter $b$	{500, 750, 1000, 1250} au
Encounter velocity $v_{\text{inf}}$	{0.5, 1.0} $\times 10^{-3} \text{ au d}^{-1}$
Initial planet semimajor axis $a$	{50, 100, 200, 400, 800} au
Initial planet pericentre $q$	{1, 10} au

The above considerations thus define a broad parameter space for capture with  $v_{\text{inf}} \sim 1 \text{ km s}^{-1} \approx 5.8 \times 10^{-4} \text{ au d}^{-1}$ , impact parameter  $b \sim 1000$  au, semimajor axis  $a \sim 1000$  au. For the mass of the original host  $M_{\star}$  we consider a range from 0.1 to  $1.5 M_{\odot}$ , covering a wide range of known planet hosts. For the eccentricity of Planet 9’s original orbit, we focus on very high values corresponding to pericentres of 1–10 au, consistent with the aftermath of a phase of strong planet–planet scattering as we describe in section 3. Our parameter choices are listed in Table 1. We explore this parameter space with N-body integrations using the MERCURY package (Chambers 1999). We use the conservative BS algorithm to integrate the trajectories of the Sun and an intruder; the latter is surrounded by an isotropic swarm of massless test particles (750 per integration). The intruder begins at 10 000 au with a velocity  $v_{\text{inf}}$ , and the system is integrated until the intruder attains a heliocentric distance of 20 000 au, at which distance bodies are removed from the integration. For each integration, we count the number of particles captured onto bound orbits around the Sun (imposing a cut-off of  $a = 5000$  au to reject particles which spuriously remain bound after removal of the original host),

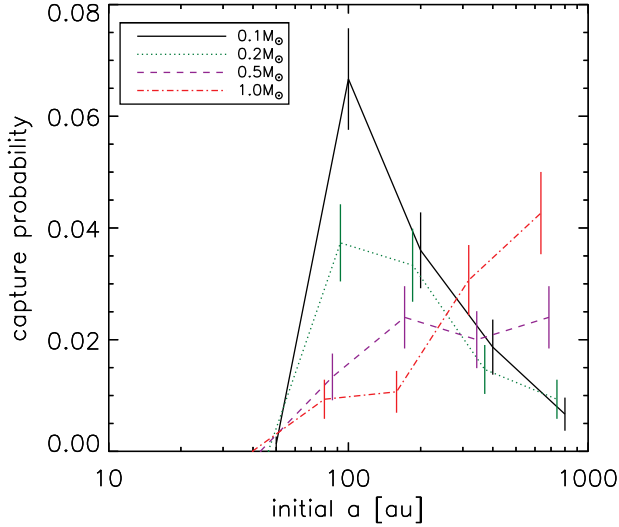


**Figure 2.** Probabilities for capture into Novenito orbits for objects on orbits of different initial semi-major axes around stars of different masses. Other parameters are fixed at bodies’ initial pericentre  $q = 10$  au, impact parameter  $b = 1000$  au,  $v_{\text{inf}} = 5 \times 10^{-4}$  au d $^{-1}$ . Note that a  $1.5 M_{\odot}$  star with these encounter parameters would disrupt the Kuiper Belt. Error bars show the  $1\sigma$  range of the posterior distribution from inverting the binomial sampling distribution. Symbols offset for clarity.

as well as the number captured onto Novenito orbits of  $a \in [400, 1500]$  au and  $e \in [0.5, 0.8]$ .

We find that the Sun can capture bodies from the intruding star for many combinations of parameters. Examples of the final orbital elements of captured bodies are shown in Figure 1. Our highest capture rate is 44%, attained for  $M_{\star} = 0.5 M_{\odot}$ ,  $b = 750$  au,  $a = 800$  au,  $v_{\text{inf}} = 5 \times 10^{-4}$  au d $^{-1}$ . However, of these captured particles, only 8% (4% of the total) have orbital elements suitable for a Novenito. Other parameter combinations give higher rates of capture into Novenito orbits, reaching 7% for  $M_{\star} = 0.1 M_{\odot}$ ,  $b = 1000$  and 1250 au,  $a = 100$  au,  $v_{\text{inf}} = 5 \times 10^{-4}$  au d $^{-1}$ ; and  $M_{\star} = 0.5 M_{\odot}$ ,  $b = 750$  au,  $a = 400$  au,  $v_{\text{inf}} = 5 \times 10^{-4}$  au d $^{-1}$ . While these are our most successful simulations, capture rates of a few percent are attained for a much wider range of parameters. Cuts through the parameter space are shown in Figure 2. Our full results are given in Table A1 of the online version of this paper.

We also ran simulations to check that the Sun’s Kuiper Belt would not be disrupted in such an encounter. For these we distributed round the Sun 750 particles at  $a = 50$  au,  $e = 0$ , with isotropic inclinations, and verified that eccentricities remained low ( $\lesssim 0.1$ ) after the flyby. These simulations ruled out impact parameters of  $b = 1000$  au and below for a  $1.5 M_{\odot}$  intruder, down to  $b = 500$  au and below for a  $0.1 M_{\odot}$  intruder, with  $v_{\text{inf}} = 5 \times 10^{-4}$  au d $^{-1}$ .

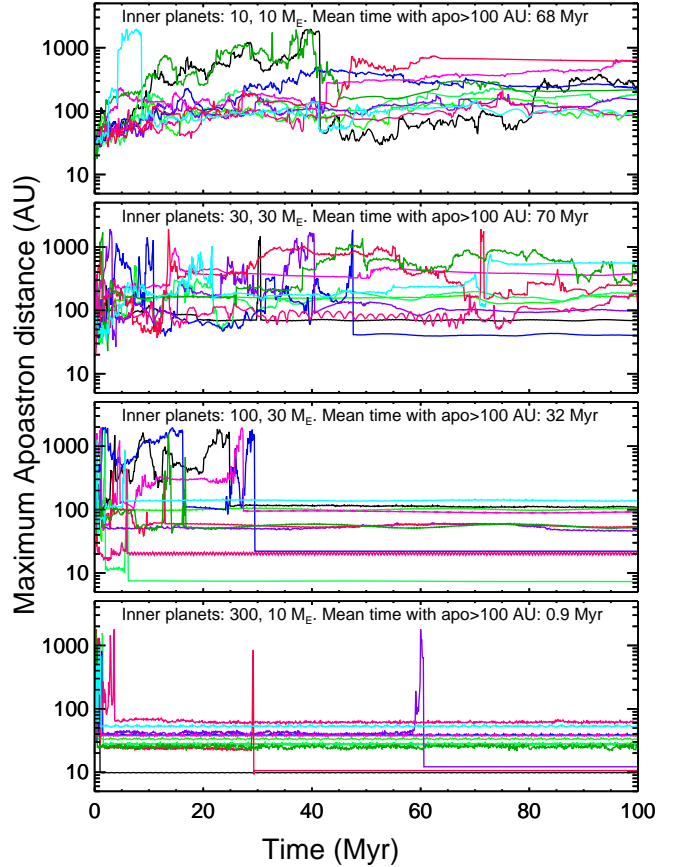


**Figure 3.** Evolution of the apocentre of the most distant bound planet in example 6-planet scattering simulations with the innermost planet at 10 au around a  $0.2 M_{\odot}$  star. Each line (10 per panel) shows the evolution in one simulation.

### 3 SOURCE POPULATIONS OF NOVENITOS

Our flyby simulations show that capture of Novenitos can occur, without disrupting the cold classical KBOs, so long as such planets exist on orbits with apastra greater than 100 au around their parent star. How common are such low-mass, wide-orbit planets? While direct imaging surveys have revealed a handful of massive super-Jovian planets on very wide orbits around young stars (e.g., Chauvin et al. 2005a,b; Lafrenière et al. 2010; Marois et al. 2010; Carson et al. 2013; Kuzuhara et al. 2013; Rameau et al. 2013; Bailey et al. 2014), the occurrence rate of lower-mass planets on wide orbits is unknown. However, in regions closer to the star the planet occurrence rate is observed to rise strongly with decreasing planet mass (Cumming et al. 2008; Howard et al. 2010; Fressin et al. 2013), while microlensing surveys probing the snow line find that  $\sim 50\%$  of low-mass stars host a snow-line planet (Gould et al. 2010; Shvartzvald et al. 2016), and we might therefore expect suitable planets to be fairly common. How might such planets attain very wide orbits? While *in situ* formation of super-Jovian planets may be possible via gravitational instability (Boss 1997; Kratter & Lodato 2016), this could not lead to the formation of Neptune- or super Earth-mass planets. One possibility would be peb-

ble accretion onto an existing core (Lambrechts & Johansen 2012), although at distances of 10s or 100s of au this may require massive discs or high dust:gas ratios (Lambrechts & Johansen 2014). Coagulation of small rocks may be possible at several hundreds of au (Kenyon & Bromley 2015), although this process takes several Gyr, far longer than the expected time for which the Sun resided in its birth cluster.

More promising may be the ejection of planets from regions closer to the star. Previous studies have shown that planets in the process of being ejected from unstable multiple systems may persist on wide orbits for extended periods of time (Scharf & Menou 2009; Veras et al. 2009; Raymond et al. 2010; Malmberg et al. 2011, Götberg et al., A&A, submitted). We run scattering simulations with the hybrid integrator of the MERCURY package to quantify more carefully the timescales on which such planets are retained on orbits that we showed above are suitable for capture by the Sun in a flyby. We take a  $0.2 M_{\odot}$  primary and study 4- and 6-planet systems of a range of masses: The inner two planets' masses range from  $10 M_{\oplus}$  to  $300 M_{\oplus}$ , while the outer planets are always assigned  $10 M_{\oplus}$  (the mass identified by Batygin & Brown 2016). Planets are initially started in unstable configurations on near-circular, near-coplanar orbits ( $e < 0.02$ ,  $i < 1^{\circ}$ ) separated by  $3.5 - 5$  mutual Hill radii, and we conduct two sets of simulations: one “pessimistic” with the innermost planet at 3 au and four planets in total and one “optimistic” with the innermost planet at 10 au and 6 planets in total. The systems are integrated for 100 Myr. Planets are considered “ejected” once their distance from the star exceeds 10 000 au (In a cluster environment, the tidal field of the cluster or perturbations from passing stars would make themselves felt at these distances, Tremaine 1993.). For each system, we record the fraction of time for which a  $10 M_{\oplus}$  planet exists with an apocentre  $Q$  beyond 100 au. Energy is always conserved to better than 2 parts in  $10^{-4}$ .

Sample orbital evolution is shown in Figure 3, for the simulations with the innermost planet at 10 au. Systems with very massive planets (Saturn–Jupiter mass) swiftly eject the lower-mass planets. In contrast, systems comprising only  $\sim$  Neptune-mass planets ( $10$  and  $30 M_{\oplus}$ ) can retain their unstable planets for many 10s of Myr. The mean durations for which systems retain planets with apocentres beyond 100 au are indicated in Figure 3, and are tabulated in Table A2 of the online version of this paper. When starting with planets on wider orbits (innermost at 10 au), we find that planets can be retained on  $Q > 100$  au orbits for most of the first 100 Myr (our best case being 75%), while with the planets starting at 3 au the planets can be retained for at most a few 10s of Myr. This can be attributed partly to the longer dynamical time-scales for the wider systems, and partly to the larger number of orbits required for ejection with lower-mass planets (see e.g. Raymond et al. 2010).

## 4 DISCUSSION

How likely is the Sun to have picked up Planet 9 in a flyby, following scattering of the planet to a wide orbit around its original host? We can estimate the probability of a successful capture as  $P_{\text{Planet9}} = P_{\text{flyby}} P_{\text{multi}} P_{\text{unstable}} f_{\text{wide}} P_{\text{capture}}$ , where  $P_{\text{flyby}}$  is the probability of the Sun experiencing a suitable flyby,  $P_{\text{multi}}$  is the probability of having a mul-

tiple planetary system,  $P_{\text{unstable}}$  is the probability of said system being unstable,  $f_{\text{wide}}$  is the fraction of the cluster lifetime that such an unstable system retains a wide-orbit planet, and  $P_{\text{capture}}$  is the probability of capturing a wide-orbit planet into a suitable orbit around the Sun. We show in Section 2 that  $P_{\text{capture}} \lesssim 7\%$ , and in Section 3  $f_{\text{wide}} \lesssim 75\%$ . Previous studies of cluster dynamics show that  $P_{\text{flyby}} \sim 1$  (Malmberg et al. 2007, 2011). The most difficult numbers to estimate are  $P_{\text{unstable}}$  and  $P_{\text{multi}}$ . An optimistic estimate draws a parallel with Jovian planets where a very high incidence of instability is required to explain the eccentricity distribution: Jurić & Tremaine (2008) find  $P_{\text{unstable}} = 75\%$ , while Raymond et al. (2011) find 83%. We may then combine this with the microlensing estimate of 50% of stars having a wide-orbit Neptune (Shvartzvald et al. 2016), and assume that all such systems are or were multiple. This gives an optimistic  $P_{\text{Planet9}} = 2\%$ . Pessimistically, we may assume that all multiple-Neptune systems are intrinsically stable (as appears to be the case for *Kepler* systems, Johansen et al. 2012); in a cluster environment however, otherwise stable systems can be destabilised by encounters with other stars, and Malmberg et al. (2011) find that  $P_{\text{unstable}} \sim 10\%$  of Solar System clones (otherwise stable) in a cluster will eject a planet within 100 Myr as a result of a close encounter. We then take  $P_{\text{multi}} = 16\%$  from Gould et al. (2010), which was based on a single detection of a two-planet system. Taking a pessimistic  $P_{\text{capture}} = 1\%$ , we then find a pessimistic  $P_{\text{Planet9}} \sim 0.01\%$ . Thus, the probability for our Planet 9 capture scenario is  $P_{\text{Planet9}} \sim 0.01 - 2\%$ , and these numbers compare favourably to the probability of a random alignment of  $7 \times 10^{-5}$  estimated by Batygin & Brown (2016). We also note that the study of Li & Adams (2016) found a probability of  $\lesssim 2\%$  for the capture of Planet 9, assuming the existence of such a body on a wide circular orbit around another star, and sampling the mass of the original host from the stellar IMF. This number corresponds to our  $P_{\text{flyby}} P_{\text{capture}}$ ; thus our studies are broadly in agreement. A better knowledge of the occurrence rate of low-mass wide-orbit planets will be needed to refine the probabilities for capture.

How might the capture scenario be confirmed or refuted? Different histories for Planet 9 may affect the distributions of orbital elements of distant TNOs in different ways. As an example, we ran a capture simulation in which a  $10 M_{\oplus}$  planet was captured from a  $0.2 M_{\odot}$  star onto an orbit of 283 au. In this simulation, the Sun already possesses a scattered disc of 750 test particles with pericentres of 40 au and eccentricities of 0 to 0.9. Following the flyby, the system was integrated for over 800 Myr. The time evolution of the longitudes of periapsis of particles, relative to that of the planet, is shown in Figure 4. Only particles with semi-major axes between 70 and 1000 au are shown. Batygin & Brown (2016) show that families of aligned and anti-aligned particles can exist under the influence of Planet 9, and in our integration a strong concentration of particles in orbits aligned with the planet is evident, together with a small number in an anti-aligned configuration. Furthermore, Jílková et al. (2016) show that if multiple bodies are captured in an encounter then they typically have similar arguments of periapsis, so if the Sun picked up planetesimals along with Planet 9 (perhaps from the “mini Oort clouds” that can accompany planet–planet scattering, Raymond & Armitage

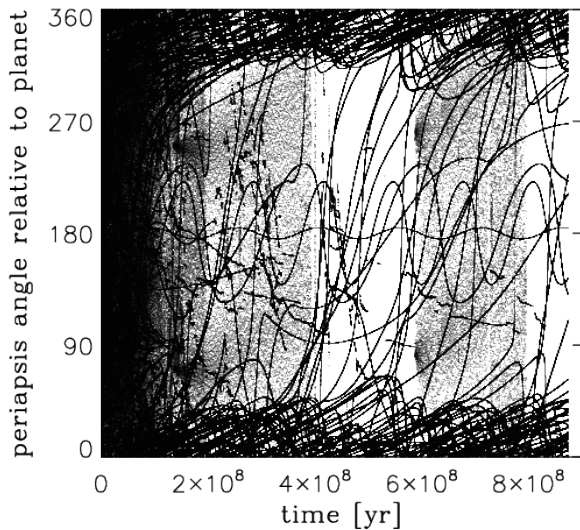


**Figure 4.** Orbital evolution of outer Solar System bodies sculpted by a captured Planet 9. We plot the longitude of periapsis of scattered disc particles between 70 and 1000 au, relative to that of the planet at 283 au. After removal of unstable particles after  $\sim 100$  Myr, a concentration of particles at  $\Delta\varpi \approx 0^\circ$  is evident, together with a smaller number in the anti-aligned configuration ( $\Delta\varpi \approx 180^\circ$ ) postulated by [Batygin & Brown \(2016\)](#) for the orientation of Sedna and similar TNOs.

2013), these would add to the aligned population. If Planet 9 should truly exist, the capture scenario would thus seem to predict a much larger population of bodies with periapsides opposite those of Sedna and its ilk. While we caution that this is based on one single example of a coplanar capture, and we have neglected the effects of the known planets, it is likely that the distribution of orbital elements of distant TNOs will in the future prove a powerful discriminant between different scenarios for emplacing Planet 9 on its orbit, such as capture, *in situ* formation, and scattering by the Solar System’s known giant planets, and we encourage further dynamical studies to explore these possibilities.

## ACKNOWLEDGEMENTS

AJM and MBD acknowledge funding from the Knut and Alice Wallenberg Foundation. SNR thanks the Agence Nationale pour la Recherche for support via grant ANR-13-BS05-0003-002 (MOJO). We are indebted to Daniel Carrera for a social media post that led to the formation of this collaboration.

## REFERENCES

Adams F. C., 2010, *ARA&A*, **48**, 47  
 Adams F. C., Proszkow E. M., Fatuzzo M., Myers P. C., 2006, *ApJ*, **641**, 504  
 Bailey V., et al., 2014, *ApJ*, **780**, L4  
 Batygin K., Brown M. E., 2016, *AJ*, **151**, 22  
 Belbruno E., Moro-Martín A., Malhotra R., Savransky D., 2012, *Astrobiology*, **12**, 754

Boss A. P., 1997, *Science*, **276**, 1836  
 Breslau A., Steinhausen M., Vincke K., Pfalzner S., 2014, *A&A*, **565**, A130  
 Brown M. E., Batygin K., 2016, preprint, ([arXiv:1603.05712](#))  
 Carson J., et al., 2013, *ApJ*, **763**, L32  
 Chambers J. E., 1999, *MNRAS*, **304**, 793  
 Chauvin G., Lagrange A.-M., Dumas C., Zuckerman B., Mouillet D., Song I., Beuzit J.-L., Lowrance P., 2005a, *A&A*, **438**, L25  
 Chauvin G., et al., 2005b, *A&A*, **438**, L29  
 Cumming A., Butler R. P., Marcy G. W., Vogt S. S., Wright J. T., Fischer D. A., 2008, *PASP*, **120**, 531  
 Fienga A., Laskar J., Manche H., Gastineau M., 2016, preprint, ([arXiv:1602.06116](#))  
 Fressin F., et al., 2013, *ApJ*, **766**, 81  
 Ginzburg S., Sari R., Loeb A., 2016, preprint, ([arXiv:1603.02876](#))  
 Gould A., et al., 2010, *ApJ*, **720**, 1073  
 Howard A. W., et al., 2010, *Science*, **330**, 653  
 Jílková L., Portegies Zwart S., Pijloo T., Hammer M., 2015, *MNRAS*, **453**, 3157  
 Jílková L., Hamers A. S., Hammer M., Portegies Zwart S., 2016, *MNRAS*, **457**, 4218  
 Johansen A., Davies M. B., Church R. P., Holmelin V., 2012, *ApJ*, **758**, 39  
 Jurić M., Tremaine S., 2008, *ApJ*, **686**, 603  
 Kenyon S. J., Bromley B. C., 2015, *ApJ*, **806**, 42  
 Kratter K. M., Lodato G., 2016, preprint, ([arXiv:1603.01280](#))  
 Kuzuhara M., et al., 2013, *ApJ*, **774**, 11  
 Lafrenière D., Jayawardhana R., van Kerkwijk M. H., 2010, *ApJ*, **719**, 497  
 Lambrechts M., Johansen A., 2012, *A&A*, **544**, A32  
 Lambrechts M., Johansen A., 2014, *A&A*, **572**, A107  
 Li G., Adams F. C., 2016, preprint, ([arXiv:1602.08496](#))  
 Linder E. F., Mordasini C., 2016, preprint, ([arXiv:1602.07465](#))  
 Luhman K. L., 2014, *ApJ*, **781**, 4  
 Lykawka P. S., Mukai T., 2008, *AJ*, **135**, 1161  
 Malhotra R., Volk K., Wang X., 2016, preprint, ([arXiv:1603.02196](#))  
 Malmberg D., de Angeli F., Davies M. B., Church R. P., Mackey D., Wilkinson M. I., 2007, *MNRAS*, **378**, 1207  
 Malmberg D., Davies M. B., Heggie D. C., 2011, *MNRAS*, **411**, 859  
 Marois C., Zuckerman B., Konopacky Q. M., Macintosh B., Barman T., 2010, *Nature*, **468**, 1080  
 Pfalzner S., et al., 2015, *Phys. Scr.*, **90**, 068001  
 Rameau J., et al., 2013, *ApJ*, **772**, L15  
 Raymond S. N., Armitage P. J., 2013, *MNRAS*, **429**, L99  
 Raymond S. N., Armitage P. J., Gorelick N., 2010, *ApJ*, **711**, 772  
 Raymond S. N., et al., 2011, *A&A*, **530**, A62  
 Scharf C., Menou K., 2009, *ApJ*, **693**, L113  
 Shvartzvald Y., et al., 2016, *MNRAS*, **457**, 4089  
 Tremaine S., 1993, in Phillips J. A., Thorsett S. E., Kulkarni S. R., eds, *Astronomical Society of the Pacific Conference Series Vol. 36, Planets Around Pulsars*. pp 335–344  
 Trujillo C. A., Sheppard S. S., 2014, *Nature*, **507**, 471  
 Veras D., Crepp J. R., Ford E. B., 2009, *ApJ*, **696**, 1600  
 de la Fuente Marcos C., de la Fuente Marcos R., 2014, *MNRAS*, **443**, L59

## APPENDIX A: ONLINE TABLES

Table A1: Numbers of particles (out of 750) captured in our flyby simulations. First three columns give the flyby parameters. Fourth column gives the particles' initial semi-major axes. Fifth and sixth columns show  $n_{\text{capt}}$ , the number of particles captured by the Sun, and  $n_{\text{Novenito}}$ , the number captured onto orbits of  $a \in [400, 1500]$  au and  $e \in [0.5, 0.8]$ , for our simulations where particles had initial pericentres of 1 au. Seventh and eighth columns show the same for initial particle pericentres of 10 au. A “-” indicates that the simulation was not run with these parameters.

$M_{\star} [M_{\odot}]$	$b$ [au]	$v_{\text{inf}} [\text{au d}^{-1}]$	$a$ [au]	$q = 1 \text{ au}$		$q = 10 \text{ au}$	
				$n_{\text{capt}}$	$n_{\text{Novenito}}$	$n_{\text{capt}}$	$n_{\text{Novenito}}$
0.1	500	$1 \times 10^{-3}$	50	46	5	44	8
0.1	500	$1 \times 10^{-3}$	100	51	9	58	8
0.1	500	$1 \times 10^{-3}$	200	32	10	26	4
0.1	500	$1 \times 10^{-3}$	400	11	2	11	3
0.1	500	$1 \times 10^{-3}$	800	4	0	3	2
0.1	750	$1 \times 10^{-3}$	50	0	0	0	0
0.1	750	$1 \times 10^{-3}$	100	1	0	6	1
0.1	750	$1 \times 10^{-3}$	200	81	13	83	10
0.1	750	$1 \times 10^{-3}$	400	30	7	37	4
0.1	750	$1 \times 10^{-3}$	800	20	5	25	2
0.1	750	$5 \times 10^{-4}$	50	201	12	182	13
0.1	750	$5 \times 10^{-4}$	100	178	23	150	19
0.1	750	$5 \times 10^{-4}$	200	68	12	96	18
0.1	750	$5 \times 10^{-4}$	400	51	9	40	7
0.1	750	$5 \times 10^{-4}$	800	14	0	14	2
0.1	1000	$1 \times 10^{-3}$	400	-	-	2	1
0.1	1000	$1 \times 10^{-3}$	800	-	-	1	0
0.1	1000	$5 \times 10^{-4}$	50	20	2	25	1
0.1	1000	$5 \times 10^{-4}$	100	205	55	192	50
0.1	1000	$5 \times 10^{-4}$	200	96	21	131	27
0.1	1000	$5 \times 10^{-4}$	400	50	9	50	14
0.1	1000	$5 \times 10^{-4}$	800	19	1	17	5
0.1	1250	$1 \times 10^{-3}$	400	-	-	1	1
0.1	1250	$1 \times 10^{-3}$	800	-	-	3	0
0.1	1250	$5 \times 10^{-4}$	50	0	0	0	0
0.1	1250	$5 \times 10^{-4}$	100	183	49	195	57
0.1	1250	$5 \times 10^{-4}$	200	111	29	121	38
0.1	1250	$5 \times 10^{-4}$	400	65	26	46	20
0.1	1250	$5 \times 10^{-4}$	800	17	3	14	1
0.2	500	$1 \times 10^{-3}$	50	22	0	34	0
0.2	500	$1 \times 10^{-3}$	100	72	4	54	8
0.2	500	$1 \times 10^{-3}$	200	39	5	35	2
0.2	500	$1 \times 10^{-3}$	400	14	3	20	3
0.2	500	$1 \times 10^{-3}$	800	-	-	6	1
0.2	750	$1 \times 10^{-3}$	50	0	0	0	0
0.2	750	$1 \times 10^{-3}$	100	0	0	6	1
0.2	750	$1 \times 10^{-3}$	200	18	1	16	3
0.2	750	$1 \times 10^{-3}$	400	16	3	20	5
0.2	750	$1 \times 10^{-3}$	800	12	4	3	0
0.2	750	$5 \times 10^{-4}$	50	191	5	129	5
0.2	750	$5 \times 10^{-4}$	100	128	8	135	21
0.2	750	$5 \times 10^{-4}$	200	75	12	75	6
0.2	750	$5 \times 10^{-4}$	400	99	9	88	7
0.2	750	$5 \times 10^{-4}$	800	54	9	74	9
0.2	1000	$1 \times 10^{-3}$	800	-	-	7	3
0.2	1000	$5 \times 10^{-4}$	50	0	0	1	0
0.2	1000	$5 \times 10^{-4}$	100	153	24	149	28
0.2	1000	$5 \times 10^{-4}$	200	104	27	115	25
0.2	1000	$5 \times 10^{-4}$	400	54	9	53	11

TableA1— continued

$M_*$ [ $M_\odot$ ]	$b$ [au]	$v_{\text{inf}}$ [au d $^{-1}$ ]	$a$ [au]	$q = 1$ au		$q = 10$ au	
				$n_{\text{capt}}$	$n_{\text{Novenito}}$	$n_{\text{capt}}$	$n_{\text{Novenito}}$
0.2	1000	$5 \times 10^{-4}$	800	39	8	39	7
0.2	1250	$1 \times 10^{-3}$	800	-	-	1	0
0.2	1250	$5 \times 10^{-4}$	100	67	21	70	19
0.2	1250	$5 \times 10^{-4}$	200	130	29	115	30
0.2	1250	$5 \times 10^{-4}$	400	72	11	54	14
0.2	1250	$5 \times 10^{-4}$	800	29	8	28	6
0.5	750	$5 \times 10^{-4}$	50	139	8	108	7
0.5	750	$5 \times 10^{-4}$	100	84	7	86	8
0.5	750	$5 \times 10^{-4}$	200	105	11	101	11
0.5	750	$5 \times 10^{-4}$	400	258	52	242	55
0.5	750	$5 \times 10^{-4}$	800	331	28	328	33
0.5	1000	$1 \times 10^{-3}$	800	-	-	21	7
0.5	1000	$5 \times 10^{-4}$	50	0	0	0	0
0.5	1000	$5 \times 10^{-4}$	100	132	10	113	10
0.5	1000	$5 \times 10^{-4}$	200	80	11	91	18
0.5	1000	$5 \times 10^{-4}$	400	107	18	99	15
0.5	1000	$5 \times 10^{-4}$	800	157	11	164	18
0.5	1250	$1 \times 10^{-3}$	800	-	-	4	0
0.5	1250	$5 \times 10^{-4}$	100	45	2	34	2
0.5	1250	$5 \times 10^{-4}$	200	94	27	79	24
0.5	1250	$5 \times 10^{-4}$	400	63	15	69	19
0.5	1250	$5 \times 10^{-4}$	800	73	8	86	12
1.0	1000	$1 \times 10^{-3}$	800	-	-	28	4
1.0	1000	$5 \times 10^{-4}$	50	1	0	6	0
1.0	1000	$5 \times 10^{-4}$	100	79	7	52	7
1.0	1000	$5 \times 10^{-4}$	200	54	9	57	8
1.0	1000	$5 \times 10^{-4}$	400	83	22	92	23
1.0	1000	$5 \times 10^{-4}$	800	191	37	193	32
1.0	1250	$1 \times 10^{-3}$	800	-	-	15	1
1.0	1250	$5 \times 10^{-4}$	100	64	5	43	1
1.0	1250	$5 \times 10^{-4}$	200	64	10	58	12
1.0	1250	$5 \times 10^{-4}$	400	60	13	54	11
1.0	1250	$5 \times 10^{-4}$	800	105	11	92	14
1.5	1250	$1 \times 10^{-3}$	800	-	-	15	4
1.5	1250	$5 \times 10^{-4}$	100	33	2	40	1
1.5	1250	$5 \times 10^{-4}$	200	56	9	48	14
1.5	1250	$5 \times 10^{-4}$	400	26	11	23	6
1.5	1250	$5 \times 10^{-4}$	800	65	15	82	16

**Table A2.** Mean durations for which systems retain planets with apastron distances  $> 100$  au. First column: masses of inner two planets. Second column: mean duration in our pessimistic case (4 planets total; innermost at 3 au). Third column: mean duration in our optimistic case (6 planets total; innermost at 10 au).

Planet mass [ $M_{\oplus}$ ]	Pessimistic duration [Myr]	Optimistic duration [Myr]
10, 10	3.7	68.0
30, 10	12.0	75.1
30, 30	21.9	69.8
100, 10	6.7	44.2
100, 30	1.6	31.9
100, 100	1.6	16.8
300, 10	0.04	0.86
300, 30	0.04	0.83
300, 100	0.09	11.6
300, 300	2.97	21.6

This paper has been typeset from a  $\text{\TeX}/\text{\LaTeX}$  file prepared by the author.